Modeling elastic wave propagation in general anisotropic media

Bas Peters, December 4 , 2012

SLIM

University of British Columbia

Elastic wave equation

σ:stress tensor, ρ:density, ω:frequency,
u:displacement, f:force, x:spatial coordinate

$$-\frac{\partial \sigma_{i,j}}{\partial x_j} - \rho\omega^2 u_i = f_i$$

Hooke's law

In Voigt notation:

$$\begin{pmatrix} \sigma_{1,1} \\ \sigma_{2,2} \\ \sigma_{3,3} \\ \sigma_{2,3} \\ \sigma_{3,1} \\ \sigma_{1,2} \end{pmatrix} = \begin{pmatrix} C_{1,1} & C_{1,2} & C_{1,3} & C_{1,4} & C_{1,5} & C_{1,6} \\ C_{1,2} & C_{2,2} & C_{2,3} & C_{2,4} & C_{2,5} & C_{2,6} \\ C_{1,3} & C_{2,3} & C_{3,3} & C_{3,4} & C_{3,5} & C_{3,6} \\ C_{1,4} & C_{2,4} & C_{3,4} & C_{4,4} & C_{4,5} & C_{4,6} \\ C_{1,5} & C_{2,5} & C_{3,5} & C_{4,5} & C_{5,5} & C_{5,6} \\ C_{1,6} & C_{2,6} & C_{3,6} & C_{4,6} & C_{5,6} & C_{6,6} \end{pmatrix} \begin{pmatrix} \frac{\partial u_1}{\partial x_1} \\ \frac{\partial u_2}{\partial x_2} \\ \frac{\partial u_3}{\partial x_3} \\ \frac{\partial u_2}{\partial x_3} + \frac{\partial u_3}{\partial x_2} \\ \frac{\partial u_3}{\partial x_1} + \frac{\partial u_1}{\partial x_3} \\ \frac{\partial u_1}{\partial x_2} + \frac{\partial u_2}{\partial x_1} \end{pmatrix}$$

Set up of linear system

- Substitute Hooke's law into the wave equation and reorganize:

$$\begin{pmatrix} A_{1,1}-\rho\omega^2 & A_{1,2} & A_{1,3} \\ A_{2,1} & A_{2,2}-\rho\omega^2 & A_{2,3} \\ A_{3,1} & A_{3,2} & A_{3,3}-\rho\omega^2 \end{pmatrix} \begin{pmatrix} u_1 \\ u_2 \\ u_3 \end{pmatrix} = \begin{pmatrix} f_1 \\ f_2 \\ f_3 \end{pmatrix}$$

$$\rightarrow [\boldsymbol{A} - \rho\omega^2 \boldsymbol{I}]\boldsymbol{u} = \boldsymbol{f}$$

- $A_{i,j}$ terms contain stiffness tensor components and spatial derivatives

Discretization

- 2nd order centred differences on 8 different coordinate systems
- This decreases the numerical dispersion and numerical anisotropy

Visualization of coordinates

- 1 Cartesian grid

a)

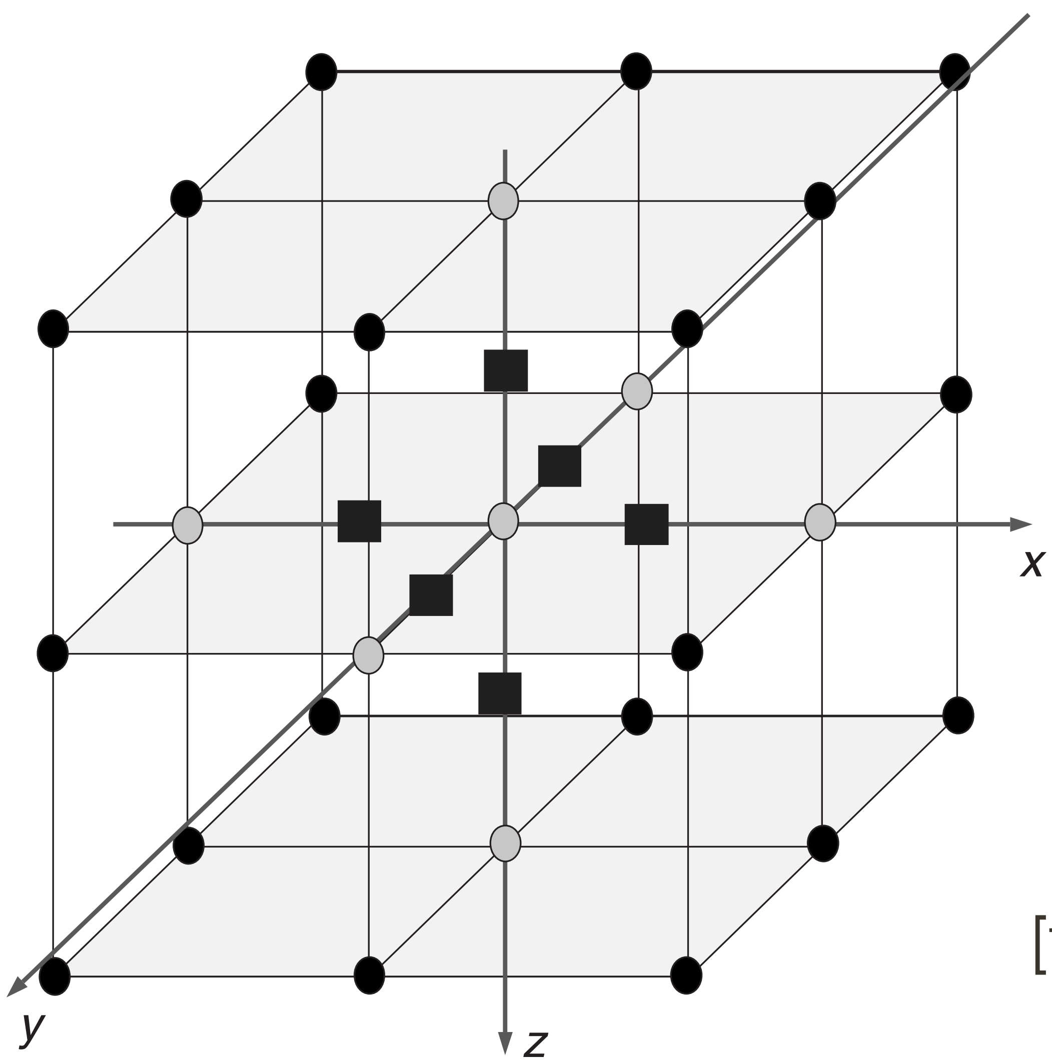

[from Operto et al., 2007]

Visualization of coordinates

- 3 coordinate systems by rotating about each of the cartesian axis

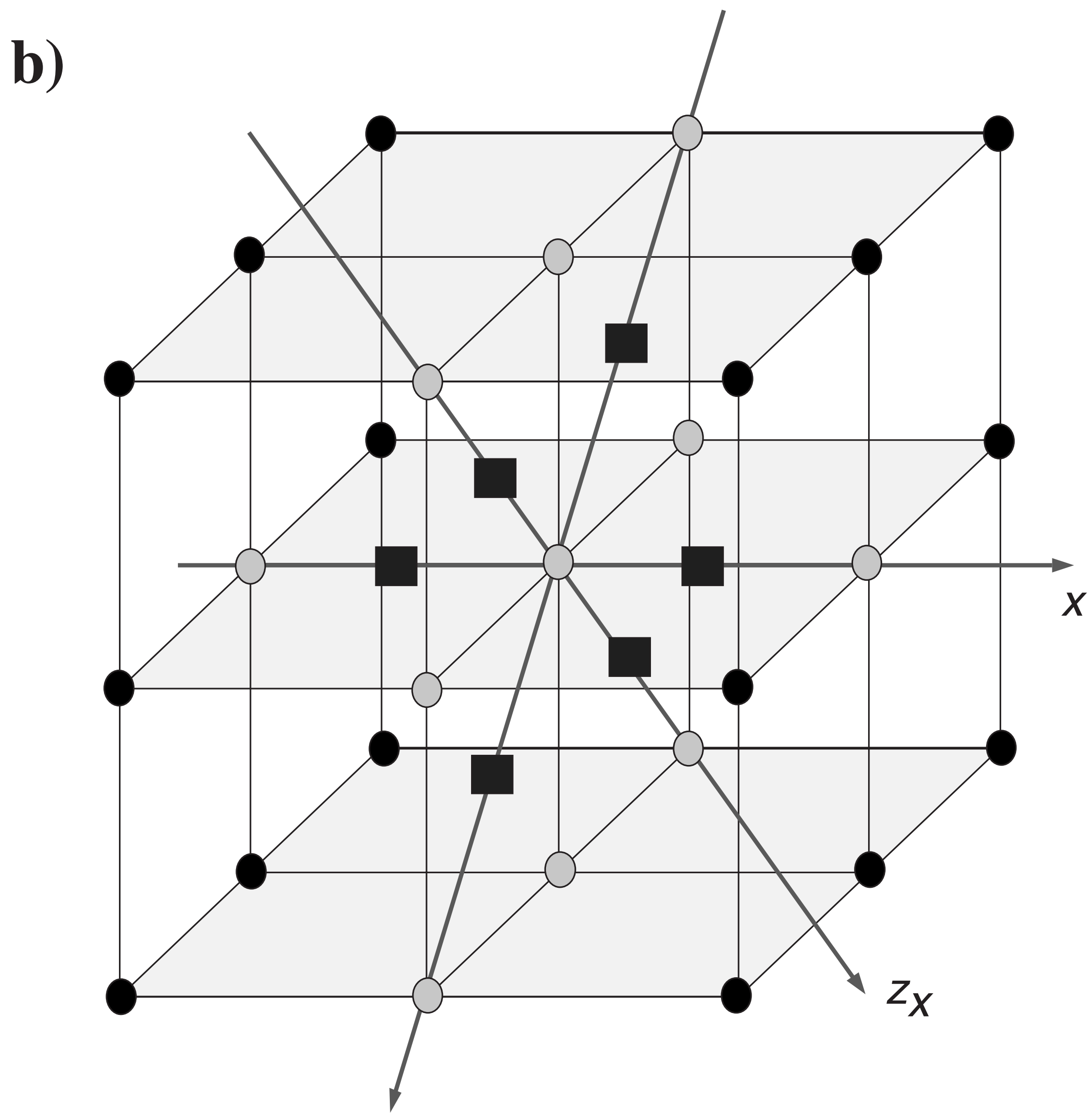

Visualization of coordinates

- 4 coordinate systems formed by 3 different diagonals of a cube

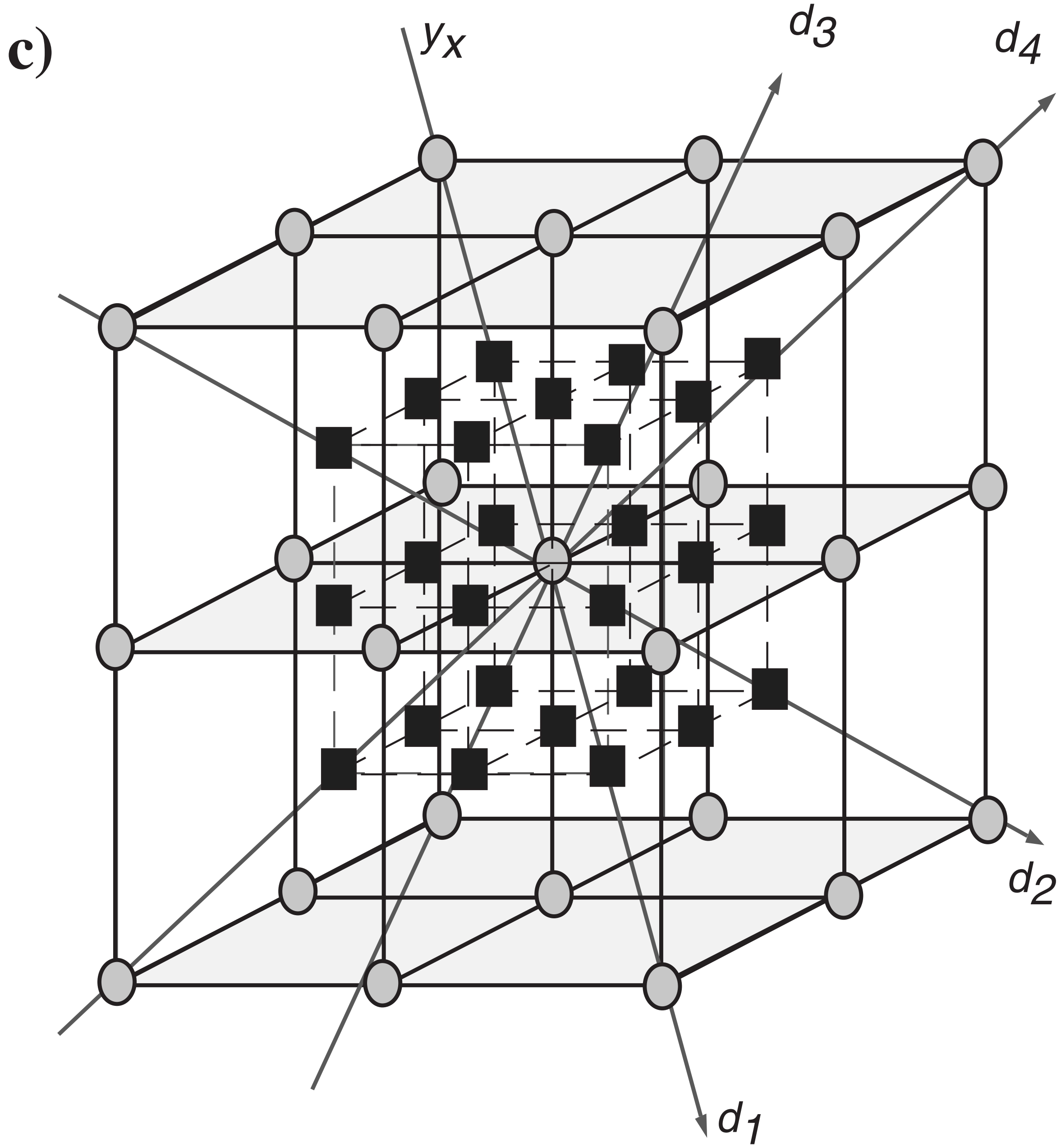

Mass lumping

- Improve accuracy by distributing the mass over grid points surrounding the grid point under consideration

SLIM

Linear combination of grids

$$\boldsymbol{A} = w_1 \boldsymbol{A}_c + \frac{w_2}{3}\left(\boldsymbol{A}_1 + \boldsymbol{A}_2 + \boldsymbol{A}_3\right) + \frac{w_3}{4}\left(\boldsymbol{A}_{d1} + \boldsymbol{A}_{d2} + \boldsymbol{A}_{d3} + \boldsymbol{A}_{d4}\right)$$

- c : Cartesian; 1,2 and 3 : rotated coordinate systems; d_1, d_2,d_3,d_4 : diagonal coordinate systems

- Estimate weights (w) by global optimization
- Results in 5 grid points per smallest wavelength

Stiffness tensor approximations

- In case modeling or estimation of all 21 components is not desired
- Example: orthorhombic symmetry:

$$\begin{pmatrix} C_{1,1} & C_{1,2} & C_{1,3} & C_{1,4} & C_{1,5} & C_{1,6} \\ C_{1,2} & C_{2,2} & C_{2,3} & C_{2,4} & C_{2,5} & C_{2,6} \\ C_{1,3} & C_{2,3} & C_{3,3} & C_{3,4} & C_{3,5} & C_{3,6} \\ C_{1,4} & C_{2,4} & C_{3,4} & C_{4,4} & C_{4,5} & C_{4,6} \\ C_{1,5} & C_{2,5} & C_{3,5} & C_{4,5} & C_{5,5} & C_{5,6} \\ C_{1,6} & C_{2,6} & C_{3,6} & C_{4,6} & C_{5,6} & C_{6,6} \end{pmatrix} \approx \begin{pmatrix} C_{1,1} & C_{1,2} & C_{1,3} & 0 & 0 & 0 \\ C_{1,2} & C_{2,2} & C_{2,3} & 0 & 0 & 0 \\ C_{1,3} & C_{2,3} & C_{3,3} & 0 & 0 & 0 \\ 0 & 0 & 0 & C_{4,4} & 0 & 0 \\ 0 & 0 & 0 & 0 & C_{5,5} & 0 \\ 0 & 0 & 0 & 0 & 0 & C_{6,6} \end{pmatrix}$$

Sparsity pattern of the system

- 81 point stencil and large bandwidth

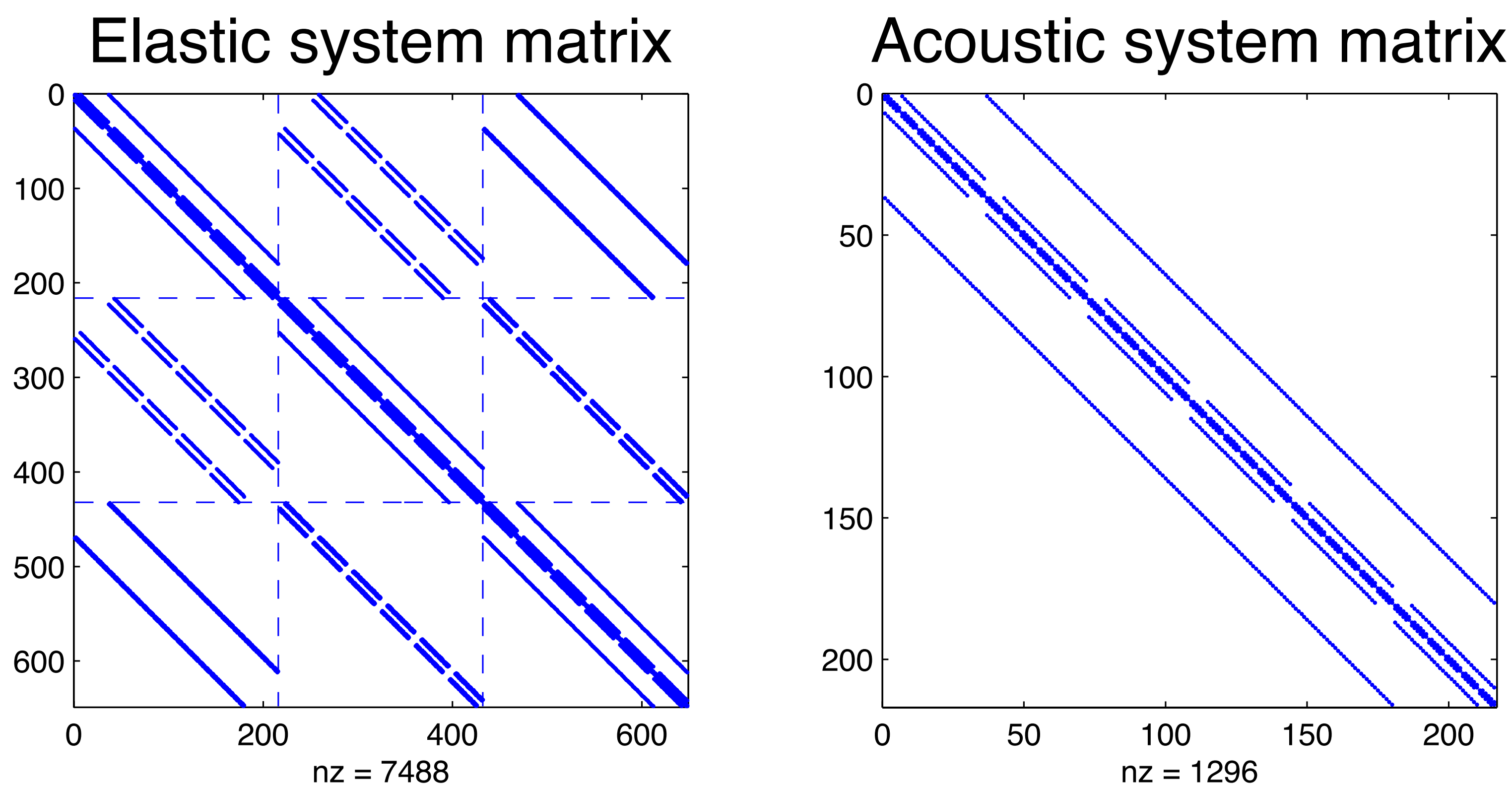

- Grid: N=(n1 x n2 x n3)
- Acoustic system = N x N , Elastic system= 3 (N x N)

System matrix permutations

1) Permute rows of $\boldsymbol{A}$ and $\boldsymbol{f}$
2) Permute columns of $\boldsymbol{A}$ and $\boldsymbol{u}$ (implicit)

$\boldsymbol{P_r}/\boldsymbol{P_c}$: row/column permutation matrix

$$\boldsymbol{P_r}\left[\boldsymbol{A}-\rho\omega^2\boldsymbol{I}\right]\boldsymbol{P_c}\,\boldsymbol{P_c}\boldsymbol{u}=\boldsymbol{P_r}\boldsymbol{f}$$

System matrix permutations

- Bandwidth is decreased a lot
- Useful for direct solvers

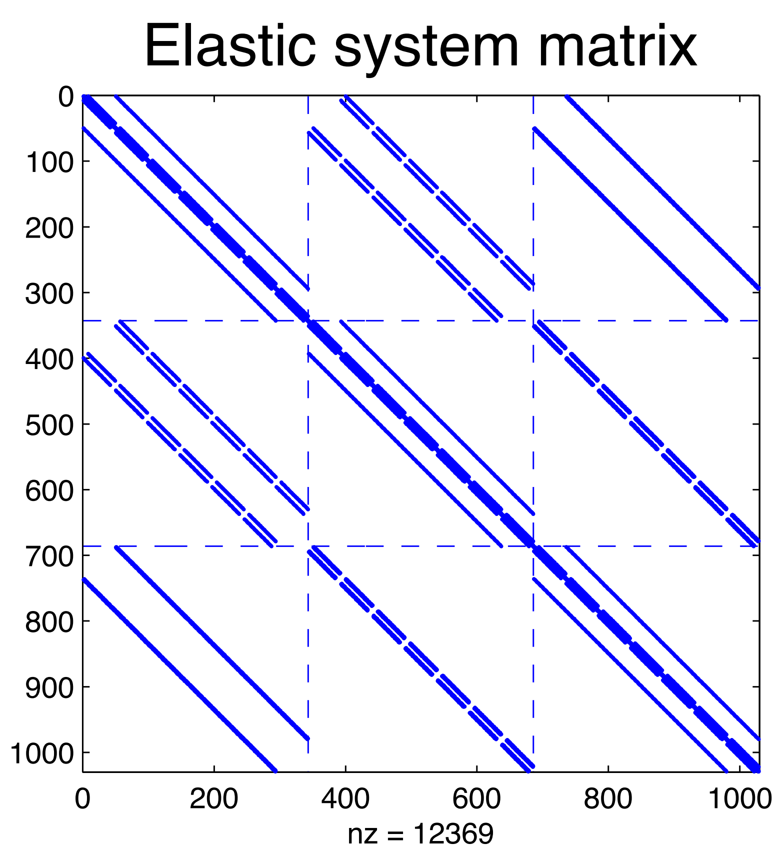

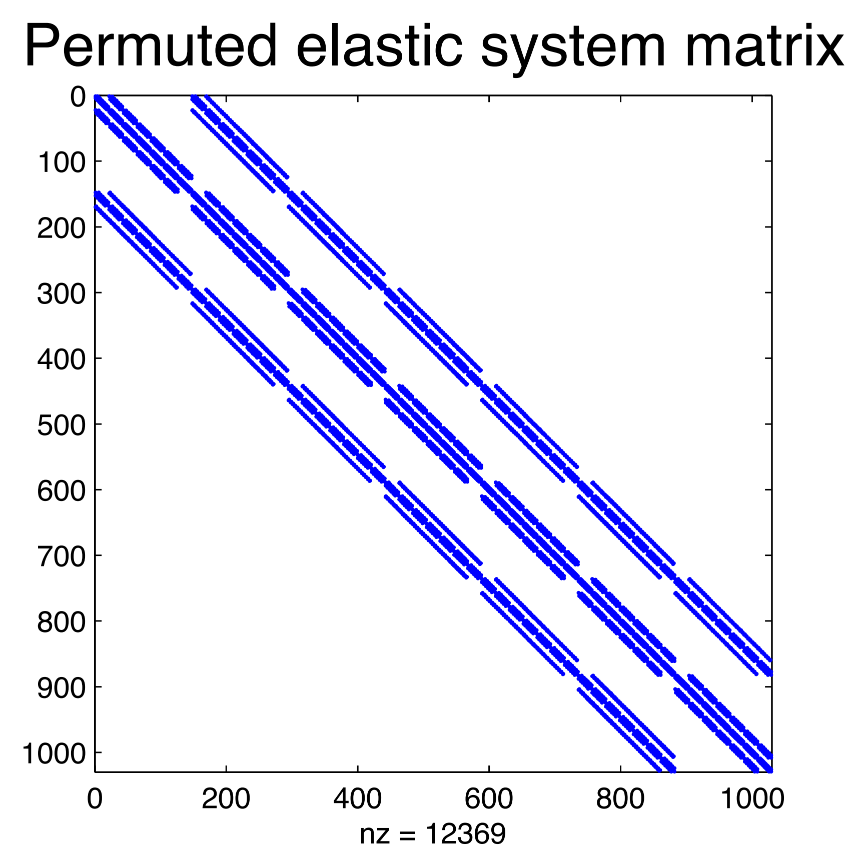

Eigenvalues

- Convergence of iterative solvers generally depends on the condition number and eigenvalue clustering
- Matrix permutation does not change the condition number, but changes the eigenvalues
- Interested in eigenvalue clustering after preconditioning, because the system matrix is indefinite

Eigenvalues

- Elastic condition number is much larger than the acoustic one
- Anisotropy can increase the condition number

- Effective preconditioner required to cluster eigenvalues/lower condition number

Solving the system

- At the moment, solve iteratively with preconditioning on CPU's
- CARPCG is currently used

Result using CARPCG

Consider (if applicable):

- Overhead cost of forming the preconditioner
- Extra matrix operations each iteration
- Number of right hand sides
- Grid size

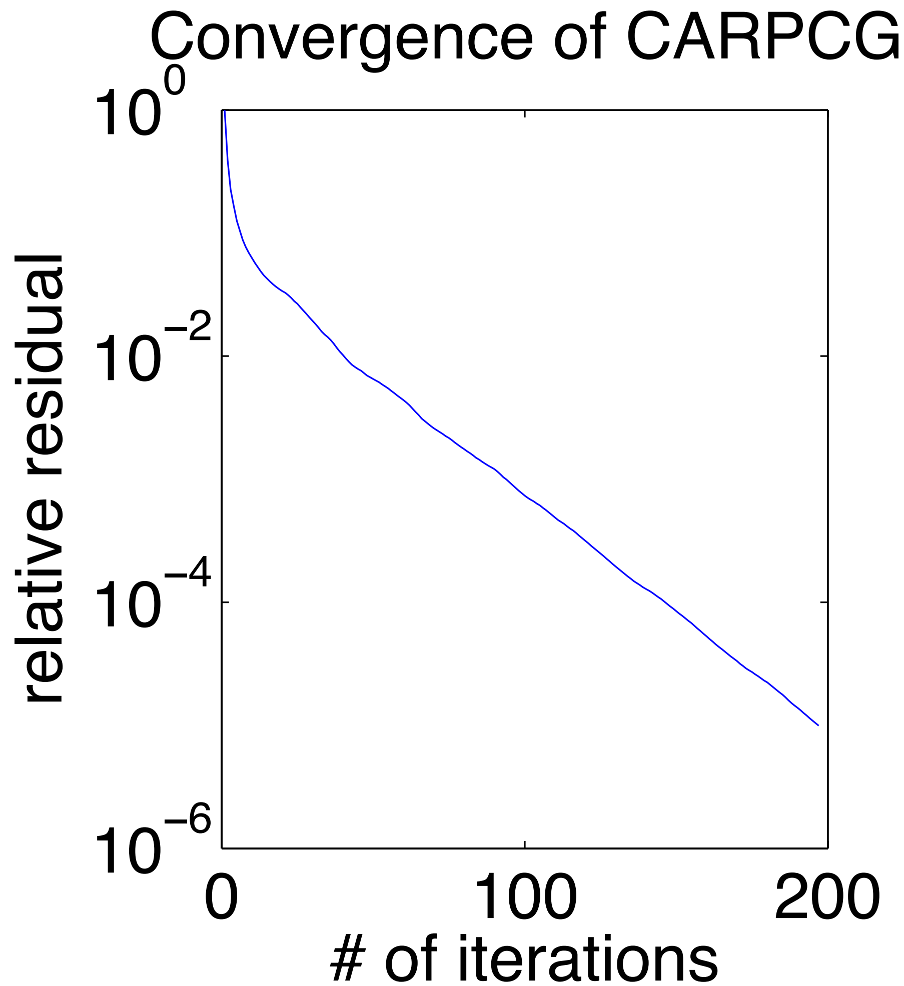

Some results

- Point force source at the center of the domain
- Energy loss and stiffness tensor are anisotropic
- Homogeneous medium with PML

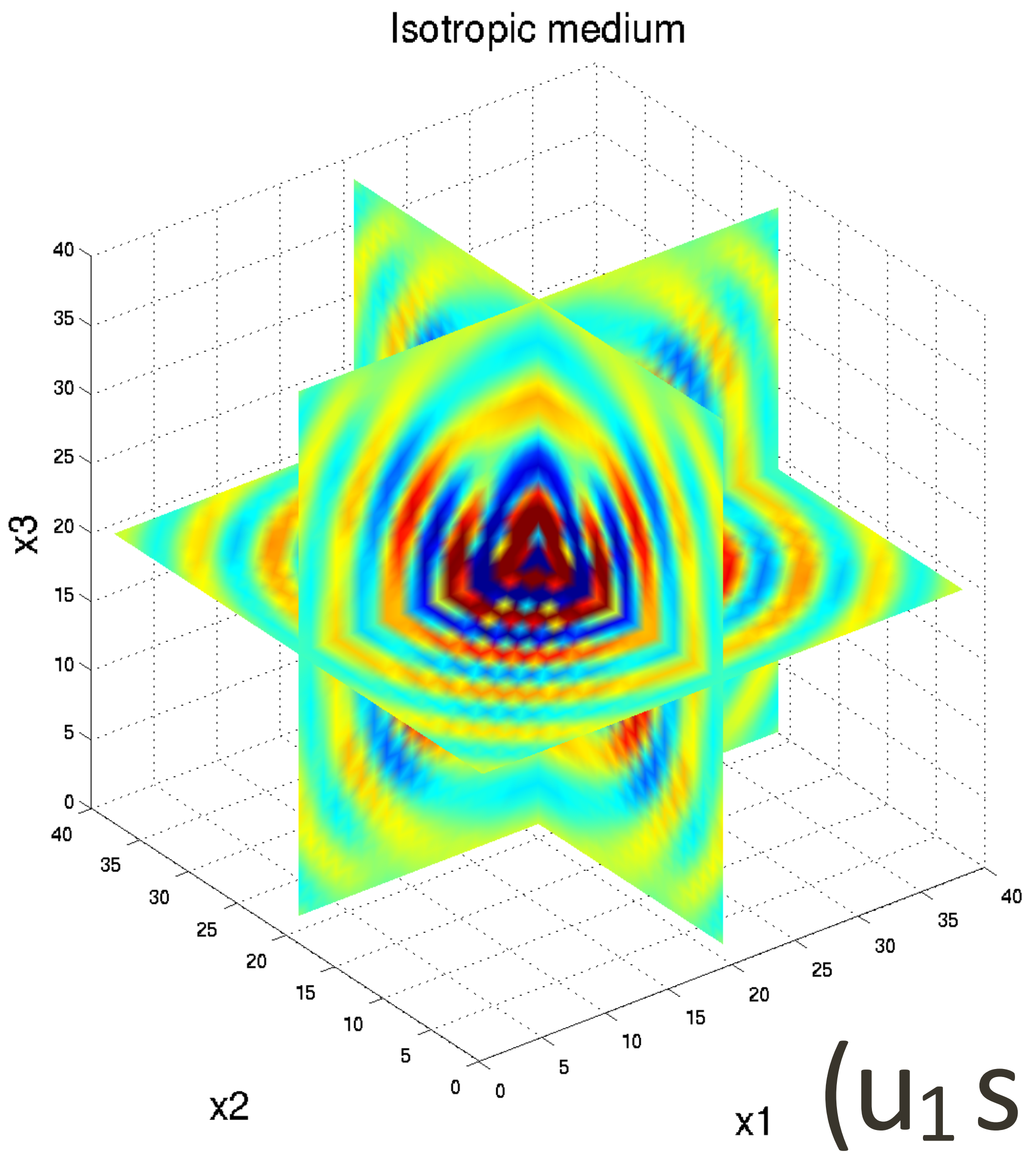

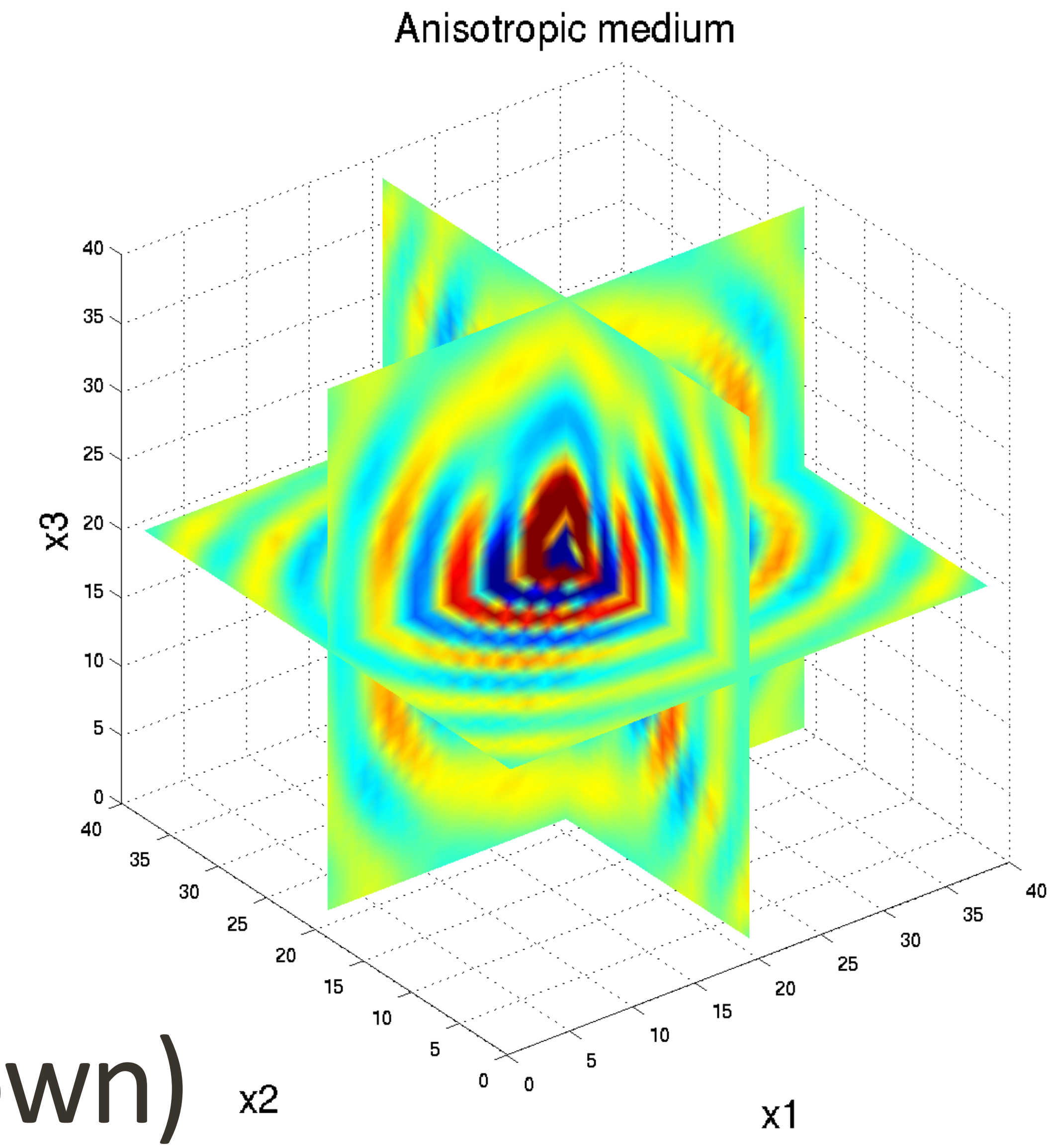

(u_1 shown)

Cross sections from previous figure

U_1 component (real part)

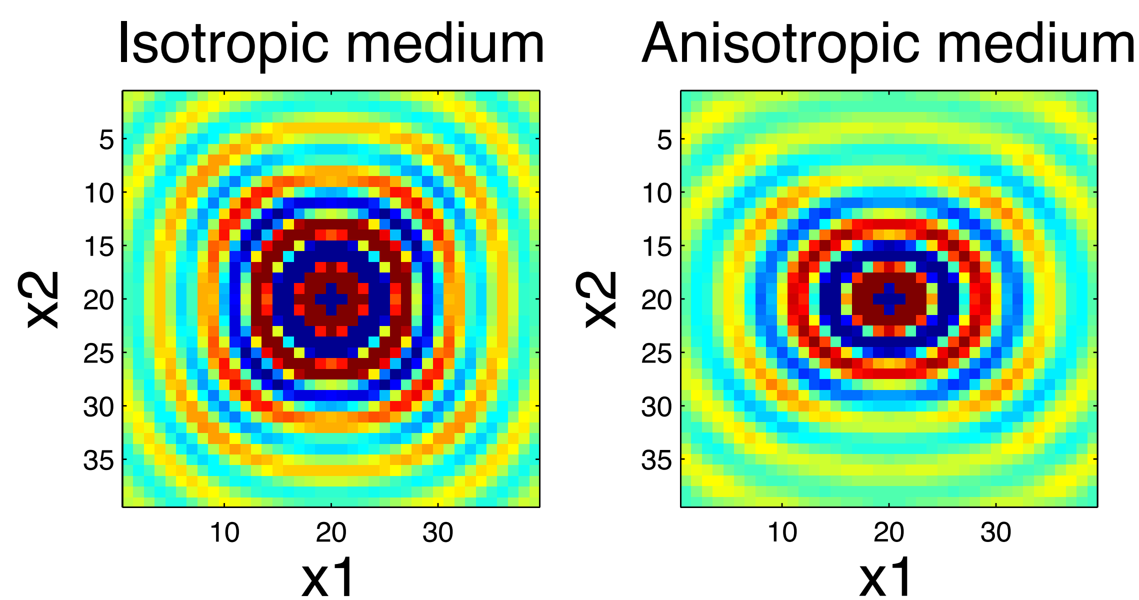

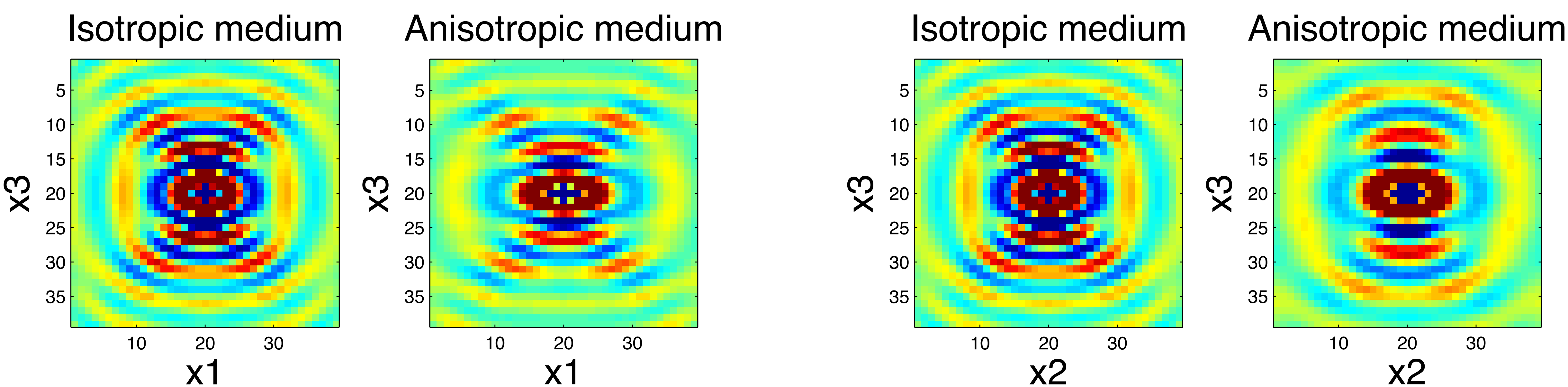

Some results

- Medium is the same as on the previous slide
- U_2 component shown this time

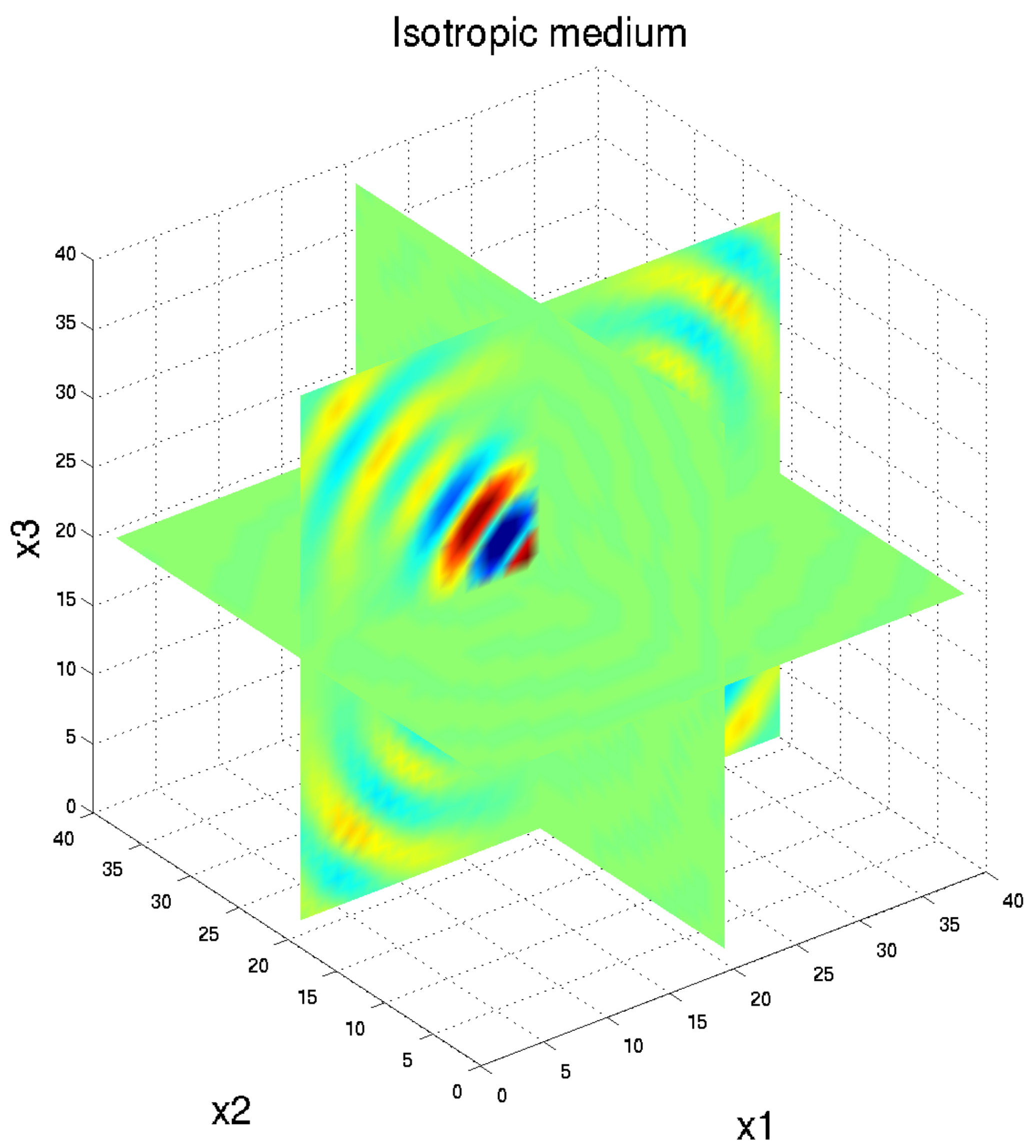

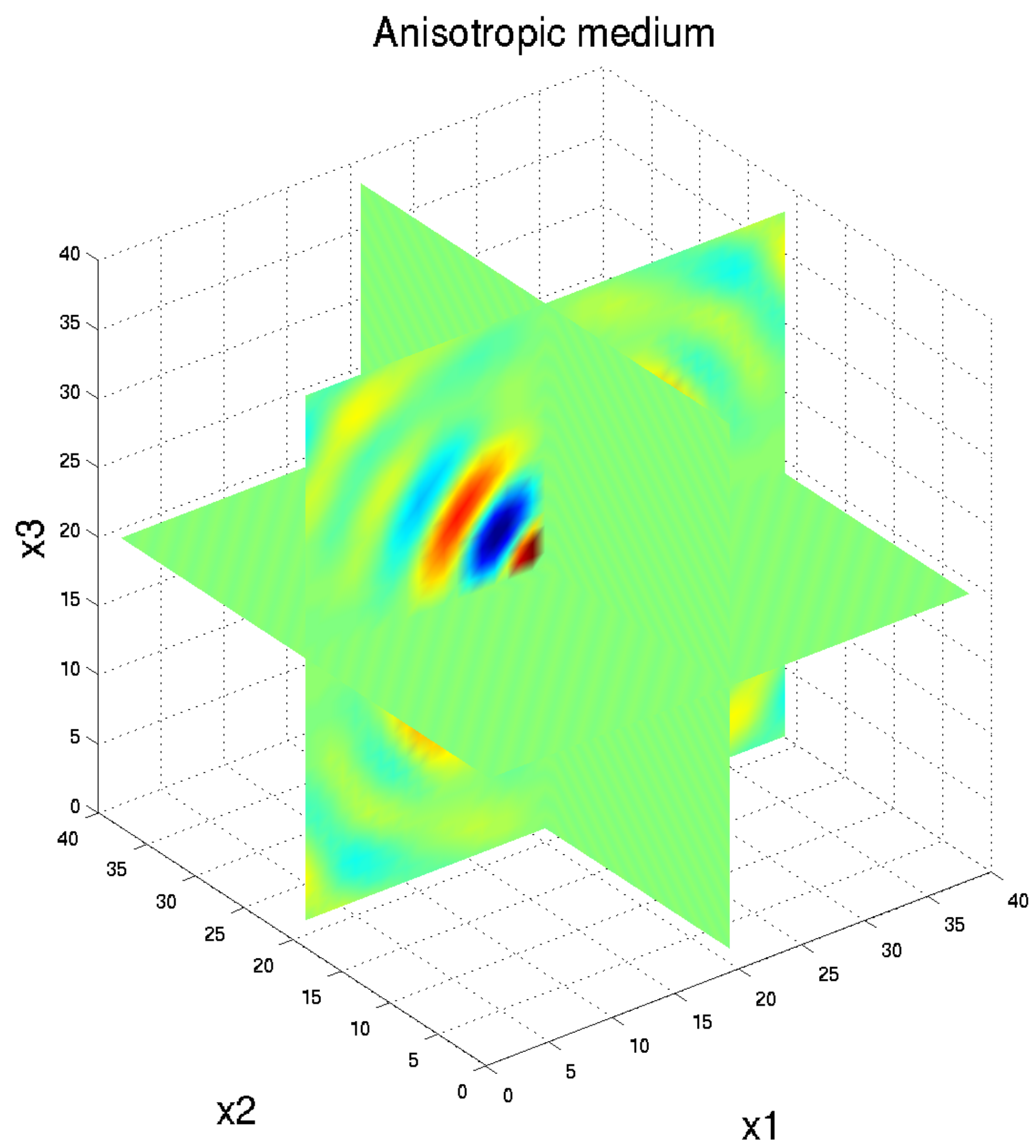

Conclusion

- Constructed a staggered finite difference scheme for solving the general anisotropic visco-elastic wave equation
- Requires a low number of grid points per wavelength

Future work

- Use in full waveform inversion by inverting for all components of the (frequency dependent) stiffness tensor (or a subset)
- Optimize *current* and develop *new* preconditioners
- Investigate which combination of discretization & linear system solver & computational hardware works the fastest

Acknowledgements

- The SLIM people

SINBAD

NSERC CRSNG

This work was in part financially supported by the Natural Sciences and Engineering Research Council of Canada Discovery Grant (22R81254) and the Collaborative Research and Development Grant DNOISE II (375142-08). This research was carried out as part of the SINBAD II project with support from the following organizations: BG Group, BGP, BP, Chevron, ConocoPhillips, Petrobras, PGS, Total SA, and WesternGeco.